

Journal of
Applied
Crystallography
ISSN 0021-8898
Editor: **Gernot Kostorz**

Formation of rocking curves for quasi-forbidden reflections in short-periodic superlattices GaAs/AlGaAs

Vasyl Kladko, Leonid Datsenko, Volodymyr Machulin, Jaroslaw Domagala, Petro Lytvyn, Jadwiga Bak-Misiuk, Andrian Kuchuk and Andrii Korchovi

Copyright © International Union of Crystallography

Author(s) of this paper may load this reprint on their own web site provided that this cover page is retained. Republication of this article or its storage in electronic databases or the like is not permitted without prior permission in writing from the IUCr.

Formation of rocking curves for quasi-forbidden reflections in short-periodic superlattices GaAs/AlGaAs

Vasyl Kladko,^{a*} Leonid Datsenko,^a Volodymyr Machulin,^a Jaroslaw Domagala,^b Petro Lytvyn,^a Jadwiga Bak-Misiuk,^b Andrian Kuchuk^a and Andrii Korchovyi^a

^aV. Lashkaryov Institute of Semiconductor Physics, NASU, 45 prospect Nauki, 03028 Kyiv, Ukraine, and ^bInstitute of Physics PAN, 32/36 al. Lotnikow, 02-609 Warsaw, Poland. Correspondence e-mail: kladko@isp.kiev.ua

Peculiarities of the diffraction patterns in short-periodic GaAlAs/GaAs superlattices were investigated in the case of quasi-forbidden reflections. The weak influence of GaAs layers on the diffraction pattern intensity, associated with a small value of an atomic form-factor difference as well as the appearance of periodic satellites, has been established. The reasons for the appearance and disappearance of the satellite structure in the diffraction patterns are discussed in relation to the structural perfection of the layers, interfacial strain and roughness of the boundaries, and layer thickness fluctuation.

© 2004 International Union of Crystallography
Printed in Great Britain – all rights reserved

1. Introduction

Significant attention is being paid to the investigation of X-ray diffraction in periodic superlattices (SLs) in connection with their unique properties. The basic method for the investigation of these objects is high-resolution X-ray diffractometry (HRXRD) (Holy *et al.*, 1998; Tapfer & Ploog, 1989). This method is used for the investigation of both technological (layer thickness) and structural characteristics of SLs, *i.e.* the level of deformation in the layers, their structural perfection, and the heterogeneity of the structure factor (Jenichen *et al.*, 1997; Bowen & Tanner, 1998; Aleksandrov *et al.*, 1998; Kyutt *et al.*, 2003). However, for short-periodic superlattices in which the thickness of the individual components of the SL's period is equal to a few monolayers, many effects of X-ray scattering have not been clarified. In particular, the physical reasons for rocking-curve (RC) satellite structure formation and the influence of sublayer thickness ratio on the intensity of satellites in the case of the so-called quasi-forbidden reflections (QFRs) (Asplund *et al.*, 2001; Datsenko *et al.*, 2002) have not been established. The reasons for the disappearance or appearance of the various order satellites for the structure and quasi-forbidden reflections also remain unknown in the general case.

The aim of this work was the investigation of the influences of structure-factor phase changes caused by the thicknesses of the layers, strains between the layers, and the structural perfection of layers, on the features of satellite formation in QFR spectra. An interpretation of the experimental diffraction patterns using numerical simulations in the framework of the semi-kinematical scattering theory is presented.

2. Theoretical and experimental procedures

When calculating X-ray diffraction patterns from a uniform epitaxial layer by the semi-kinematical theory (Holy *et al.*,

1998), the following parameters are usually used in SL structures: the layer thickness t , the Fourier coefficient of polarizability χ_h , which is known to be proportional to the structure factor F_h , and the strain. The total amplitude of X-ray scattering from a composite multilayer system can be described by the structure factor having the following form (Speriosu & Vreelang, 1984; Magilyanski *et al.*, 1999):

$$F(\mathbf{h}) = F_{\text{Cap}}(\mathbf{h}) + F_{\text{ML}}(\mathbf{h}) \exp(-i\mathbf{h}t_{\text{Cap}}) + F_{\text{B}}(\mathbf{h}) \exp[-i\mathbf{h}(t_{\text{Cap}} + t_{\text{ML}})] + F_{\text{Sub}}(\bar{h}) \exp[-i\mathbf{h}(t_{\text{Cap}} + t_{\text{ML}} + t_{\text{Buf}})]. \quad (1)$$

Here, t_{Cap} , t_{ML} and t_{Buf} are the thicknesses of the cap, total SL and the buffer layers, respectively; \mathbf{h} is the diffraction vector. The exponential factors in equation (1) allow the phase change of the scattering amplitude during propagation of X-rays through the sublayers to be described. When performing corresponding calculations, the effect of the layer thickness fluctuations Δt_i can be taken into account using the corresponding phase factor:

$$\varphi_i = \exp[-h^2(\Delta t_i)^2]. \quad (2)$$

The expression for the amplitude scattering coefficient (ASC) of coherently scattered waves in the SL in the case of homogeneous defect distribution in periodically repeating layers of two types, which are characterized by the interplane distance d , scattering ability, σ , and value of the static Debye–Waller factor E , can be written for the symmetric diffraction case as follows (Punegov, 1995):

$$R^C = iF_{\text{ML}} \exp(i\Psi) \frac{\sin(Ny)}{\sin(y)}, \quad (3)$$

where $y = A_a t_a + A_b t_b$, $A_{a,b} = (\eta + 2\pi\Delta d_{a,b}/d^2)/2$, $t_{a,b}$ is the layer thickness, $T = t_a + t_b$, $\eta = (2\pi/\lambda \sin\theta)(\chi_0 + \sin 2\theta\Delta\theta)$ is the

angular variable that characterizes a crystal orientation relative to the incident wave, $\Delta\theta = \theta - \theta_0$. θ_0 and N are the Bragg angle and number of SL periods, respectively. Here, $\Psi = (N - 1)y + A_a t_a$ stands for SL phase factor. The structure factor F_{ML} for one period is determined by

$$F_{ML} = \sigma_a E_a \frac{\sin(A_a t_a)}{A_a} + \exp(iy) \sigma_b E_b \frac{\sin(A_b t_b)}{A_b}, \quad (4)$$

where $\sigma_h = \pi \chi_h C / (\lambda \sin \theta)$ is the scattering parameter. C , χ_h and $E_{a,b}$ are polarization factor, Fourier susceptibility coefficient and the static Debye–Waller factors for layers a (GaAs) and b (AlAs or AlGaAs), respectively.

The average interplane distance for the SL period is $d = (d_a t_a + d_b t_b) / T$. The values of interplane distance deviations from an average value for each layer are determined as $\Delta d_{a,b} / d$, where $\Delta d_{a,b} = d_{a,b} - d$.

The sine denominator in the equation (3) gives rise to peaks at

$$A_a t_a + A_b t_b = n\pi, \quad (5)$$

which are denoted as n th-order satellites ($n = 0, \pm 1, \pm 2 \dots$). The SL period can be determined from the angular spacing $\Delta\theta_p$ between these peaks:

$$T = t_a + t_b = \frac{\lambda |\gamma_h|}{\Delta\theta_p \sin(2\theta_B)}. \quad (6)$$

The angular distribution of the coherently scattered intensity can be characterized by the well known Laue interference function:

$$I^C(\Delta\theta) = |F_{ML}|^2 \exp(-2 \text{Im}\Psi) \left| \frac{\sin(Ny)}{\sin(y)} \right|^2. \quad (7)$$

In the general case of numerical analysis, for comparison with the experimental data, account needs to be taken of the influence of the defects on the coherent and diffuse parts of the intensity, which arises due to structural defects in one

layer. The intensity of the diffuse scattering component can be written as (Punegov, 1995):

$$I_1^d = 2[\sigma_a^2(1 - E_a^2)\tau_{a,t_a} + \exp(-\mu t_a)\sigma_b^2(1 - E_b^2)\tau_{b,t_b}]. \quad (8)$$

Here, $\tau_{a,b}$ is the Kato correlation parameter length describing the degree of short-range ordering in the corresponding SL layer.

Using the average absorption coefficient $\mu = (\mu_a t_a + \mu_b t_b) / T$ in one SL period, the angular distribution of the diffuse scattering intensity for the SL in the vicinity of the Bragg reflection can be described using the following expression:

$$I^d(\Delta\theta) = NI_1^d \exp[-\mu T(N - 1)/2]. \quad (9)$$

The consideration of the scattering by the buffer and cap layers as well as by the substrate complicates the task. It is necessary to take into account the thickness of such layers and the phase relations in expressions for the ASC.

The zero-order SL peak deviates from that of the substrate peak by the angle $\Delta\theta_0$:

$$-\Delta\theta_0 = \tan\theta_B \langle \varepsilon_{\perp} \rangle, \quad (10)$$

where $\langle \varepsilon_{\perp} \rangle = \Delta a / a$ is the relative change of the lattice period along the growth direction, and $\langle \dots \rangle$ indicates averaging over the SL period (Holy *et al.*, 1998; Tapfer & Ploog, 1989). The structure factor for 200 QFR (which is known to be proportional to the difference between the Ga and As atomic scattering factors) is rather small in the case of this two-layer system when one of its layers is built over GaAs.

If one neglects the absorption and the contribution from a substrate, as well as the contribution to the scattering from $I^d(\Delta\theta)$, the expression for the normalized intensity for structures with a centre of symmetry can be written as follows:

$$R = |F_{ML}|^2 = \left[\sigma_a E_a \frac{\sin(A_a t_a)}{A_a} + \cos(y) \sigma_b E_b \frac{\sin(A_b t_b)}{A_b} \right]^2. \quad (11)$$

Taking into account a small contribution to the reflectivity from the GaAs layer, one may obtain the following simple expression:

$$R \simeq |F_{ML}|^2 = \cos^2(y) \left[\sigma_b E_b t_b \frac{\sin(A_b t_b)}{A_b} \right]^2. \quad (12)$$

The rocking curves for the 400 and 200 reflections of Cu $K\alpha$ radiation were recorded by the triple-crystal X-ray diffractometer (Philips MRD, Institute of Physics, Warsaw) equipped with a $4 \times \text{Ge}(220)$ monochromator and $2 \times \text{Ge}(220)$ analyser. The studied samples were scanned near the Bragg angle over a range of $\sim 3^\circ$ in the so-called $\omega/2\theta$ mode, as well as in the sample-scanning mode. The measurements were carried out with a $2''$ step increment. When analysing the experimental data obtained, the traditional χ^2 technique was used for calculations (Afanas'ev *et al.*, 1997). It enabled us to obtain both of the above-mentioned average parameters as well as their spread. Two types of short-periodic SLs grown by the molecular beam epitaxy (MBE) method were investigated, namely: 50-period GaAs (8 ML)/AlAs (4 ML) (ML here

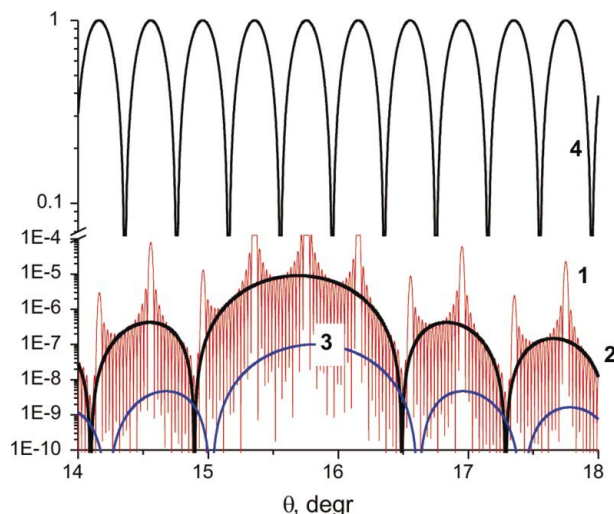


Figure 1
Calculation of the 200 rocking curve (curve 1) for the GaAs/AlAs structure, with the sine (2 and 3) and cosine (4) factors in equation (11).

Table 1

Parameters of studied structures.

Sample number and reflection	<i>a</i> , <i>b</i> sublayer thicknesses (nm)	SL period <i>T</i> (nm)	Calculated strain for a relaxed lattice $(\Delta a/a)_{m\perp}$	Experimental data according to expression (15), $(\Delta a/a)_{b\perp}$	Roughness of SL sublayer in interface (nm)
SL 8/4 (1), 200	2.248, 1.107	3.355	0.00132	0.0036	0.3
SL 8/4 (2), 400	2.245, 1.112	3.346	–	0.0032	0.4
SL (3) 6 nm/14.5 nm, 200	6.4, 15.1	21.5	–	0.00065	–
Errors	±0.002	±0.002	–	±0.00003	±0.01

denotes a monolayer) and 100-period GaAs/GaAlAs, with sublayer thicknesses of 6 and 14.5 nm, respectively.

3. Results and discussion

First, let us analyse the behaviour of the RC simulated according to equation (11) for the case of an SL with sublayers of equivalent thickness (Fig. 1, curve 1). Two ranges with different periods of *Pendelösung* oscillations could be marked. The cosine function in equations (11) and (12) describes the SL period (curve 4) and the sine function corresponds to the sublayer thickness and the contribution to the reflection power from both the AlAs (curve 2) and the GaAs sublayers (curve 3). It is easy to see that the GaAs sublayer contribution to the ASC is two orders of magnitude smaller in comparison with that of AlAs due to the very small value of the GaAs structure factor for 200 QRF. Thus, the possibility exists to determine the SL period as well as the thickness of each sublayer from a simple angular analysis of the RC shape.

Based on the above, one can write the following expression for *T* from the positions of two peaks:

$$t_a + t_b = \frac{\lambda}{2(\sin \theta_{n+1} - \sin \theta_n)}. \quad (13)$$

The sine function in equation (3) also has minima, but of its own angular periodicity 2π . So one can obtain a value for *t_b*:

$$t_b = \frac{\lambda}{\sin \theta_2 - \sin \theta_1}. \quad (14)$$

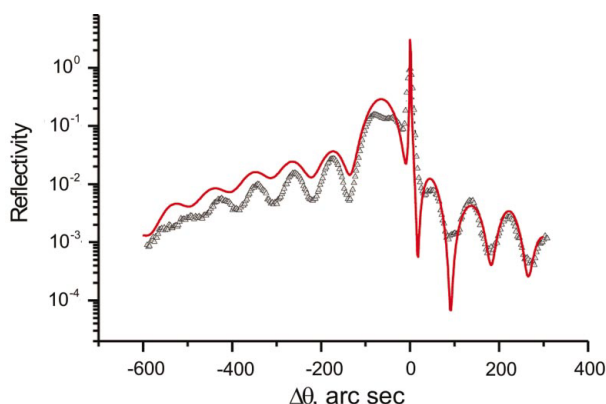


Figure 2
Experimental (points) and simulated (solid line) rocking curves for QRF 200 (ω scanning mode).

Here, θ_1 and θ_2 denote angular positions of neighbouring peaks in this RC. Using the expressions (Macranger *et al.*, 1988; Haase *et al.*, 1998), one can obtain the value of the strain in the direction normal to the crystal surface $(\Delta a/a)_{b\perp}$, at the interface between two layers:

$$\frac{t_a + t_b}{1 + (\Delta a/a)_{m\perp}} = t_a + \frac{t_b}{1 + (\Delta a/a)_{b\perp}}, \quad (15)$$

where $(\Delta a/a)_{m\perp}$ is the calculated lattice mismatch for two layers in a relaxed state.

The experimental and calculated rocking curves for the first SL-type sample studied here using QFR 200 are presented in Figs. 2 (ω scans) and 3 ($\omega-2\theta$ scans). One can see that both of these diffraction curves demonstrate not only distinct satellite structure that is determined by the SL period, but also fine interferential details. There is also rather good agreement between the fine structures of the experimental and the theoretical RCs. This is related to the values of the intensities near the zero-order satellite and its maximum positions.

It was possible to obtain some quantitative results concerning the SL parameters by using a procedure (Holy *et al.*, 1990) to fit the theoretical semi-kinematical curves to the experimental ones (points) in Figs. 2 and 3. One may also compare these results with those derived from the simple equations (13)–(15). The data obtained here by the two practically independent approaches correlate rather well. This fact indicates that our assumption concerning the small diffuse

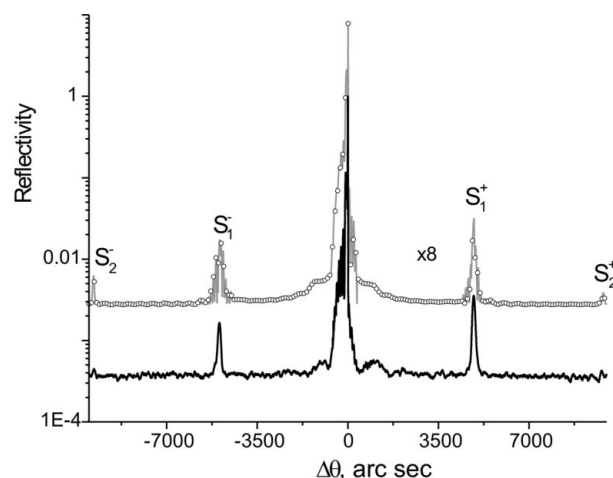


Figure 3
Rocking curves for 200 QRF ($\omega-2\theta$ scans) from SL: experimental (bottom) and simulated (upper). S^+ and S^- denote the first- (S_1) and second- (S_2) order satellites, respectively.

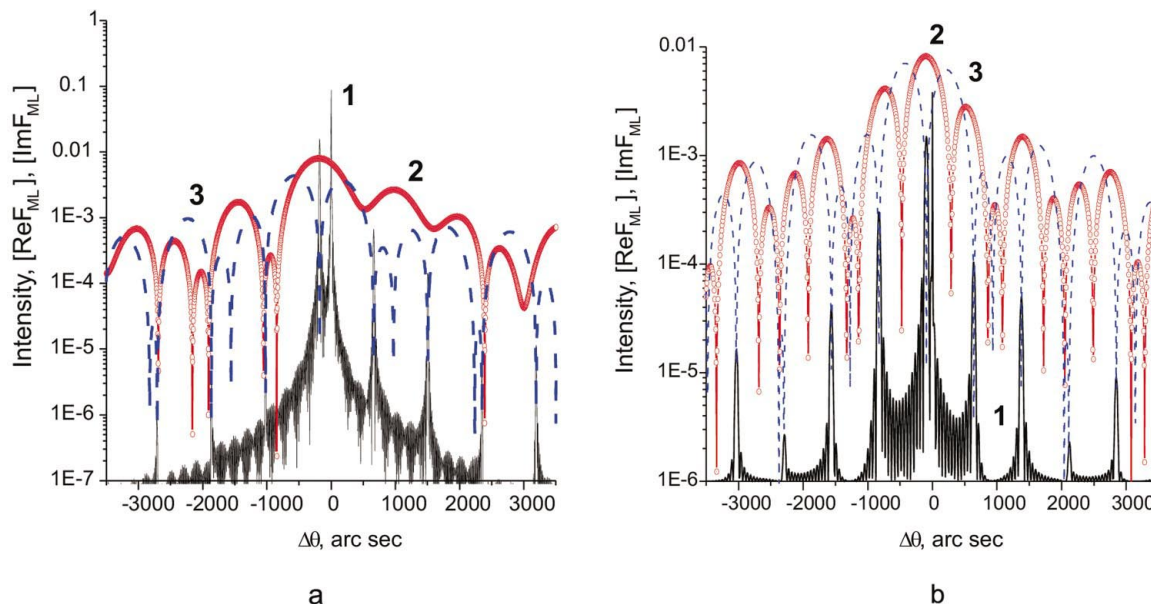


Figure 4 400 (a) and QFR 200 (b) rocking curves (1) calculated for AlGaAs and GaAs layer thickness ratio 2:1. Curves 2 and 3 are the ReF_{ML} and ImF_{ML} functions, respectively.

component contribution of the QFR 200 maxima to the X-ray scattering is valid. The results of our measurements and calculation of the SL parameters are given in Table 1. Summing up all of these results, one can state that the contribution to the QFR intensity from a layer composed of *a* and *b* components with close atomic numbers (GaAs) is rather small. Thus, the *b* layer, consisting of components with considerably different atomic numbers, mainly determines the shape of the 200 scattering patterns.

The simulations show that the variation of the period thickness affects the angular positions of the satellites and

their intensities. The third-order satellite disappearing in Fig. 4 is seen for the sublayer thickness ratio $t_b/t_a = 2$. Besides, the intensity of satellites of various order can both increase and weaken even in perfect SL structures. In order to discover the principal causes of this phenomenon, we shall consider the behaviour of real (ReF_{ML}) and imaginary (ImF_{ML}) parts of the SL structure factor (4). In Fig. 4, the simulated RCs for the SL 400 and 200 reflections are shown for comparison with the $Re_{ML}F$ and $Im_{ML}F$ variations. As can be seen, the ratio between these two parts of the structure factor determines the presence or disappearance of satellites of various order. The diffraction peaks are observed exactly at those angles where (ReF_{ML}) reaches a maximum.

The results for the SL with sublayers of equal thickness differ from those shown in Fig. 4. In this case, the second-order satellites disappear (especially for the QFR case). These results allow the formulation of a quantitative criterion of satellite disappearance, depending on the thickness ratio of the SL layers. It can be written as the following empirical formula:

$$m = p(t_a/t_b + 1), \tag{16}$$

where *p* is an integer, 1, 2, ..., and *m* is the order of the disappearing satellite.

Using the second example, we shall consider the behaviour of the satellite system in the experimental spectra (Fig. 5) for the 400 (1) and 200 (2) reflections taken from the second type of SL with a 2:1 ratio of layer thicknesses. One can see the satellites of the zeroth, first, second and third orders (positive) for the 400 reflection, allowed by the corresponding structure factor. Even more satellite structure is discovered for the 200 reflections, where both of the negative and positive satellites of the allowed orders are detected.

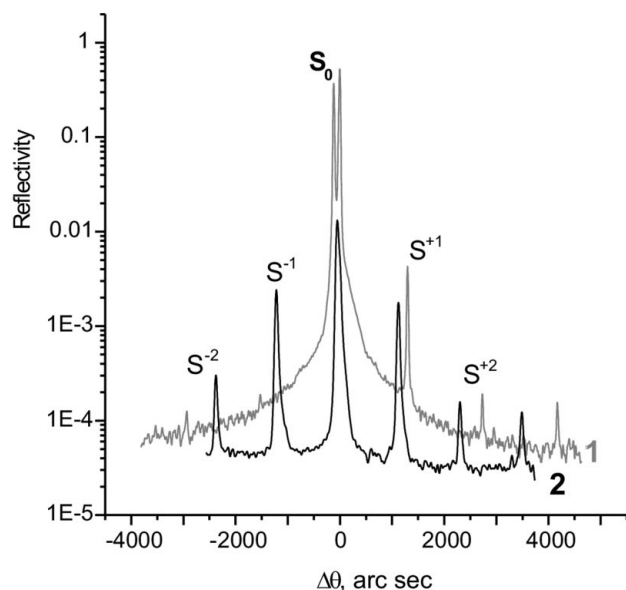


Figure 5 400 (1) and QFR 200 (2) experimental rocking curves for the 2:1 thickness ratio of AlGaAs and GaAs layers.

Another important reason for the formation of the satellite system is the structural perfection of separate SL layers. As has been shown earlier (Punegov, 1990; Kladko *et al.*, 2003), the pattern of the obtained satellite system for structure reflections depends strongly on the presence of defects in the SL layer, even in the case of good instrumental resolution. These effects are usually seen both for the structure reflections and for quasi-forbidden reflections (Velling *et al.*, 1998; Kladko *et al.*, 2001, 2003; Tran *et al.*, 2003). Our calculations show, however, that the presence of defects in the gallium arsenide layer does not practically affect the satellite intensity. This conclusion is in agreement with the data reported earlier concerning the weak influence of defects on QFR intensity in massive monocrystals (Cockerton *et al.*, 1989; Datsenko *et al.*, 2002). Thus, the influence of a perfect GaAs layer ($E = 1$) in the case of QFR is indistinguishable from the same layer with a completely amorphous structure ($E = 0$). The GaAs layer plays an important role, however, in the oscillating behaviour of the SL diffraction spectra as a phase object of a certain thickness.

For the AlAs layer, the influence of structural defects on the intensity of the satellites appears appreciable, as shown in calculations in which the static factor E varies within the limits $0 \leq E \leq 1$. Thus, the use of QFRs allows one to study separately the structural perfection of one of the SL sublayers (AlAs, for example), which is an essential advantage of the given approach in comparison with application of only the 400 structure reflection. The fitting procedure (adjustment of calculated spectra to the experimental spectra) has shown that the surface irregularity of interfaces considerably smears out the diffraction pattern, especially in the angular region of higher order satellites (Fig. 6). This outcome of the calculations is in agreement with the experimental RC (Fig. 3), where lowering of the intensity of the second-order satellites S_2 is observed. The first-order satellites and the zeroth-order satellite display a weaker sensitivity of this parameter to structural imperfections. The magnitude of statistically distributed heterogeneities of an interface between beds of an

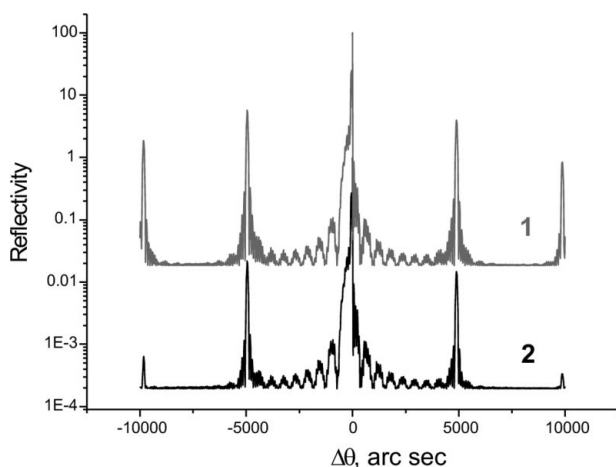


Figure 6
The simulated rocking curves for QRF 200 in the case of ideally smooth layers (1) and with roughness 0.3–0.4 nm (2).

SL amounts approximately to 0.3–0.4 nm. It is also necessary to note that asymmetry in the values of the intensities of the satellite maxima (on the left and right sides of a zero maximum) is observed only when the structure violations of both types (interplane distance modification and reflectivity variation) exist.

4. Conclusions

Quantitative agreement between the experimental and calculated diffraction patterns for QFRs is found by summing up all the results obtained. Utilization of these reflections for the determination of SL structure parameters was shown to have several advantages over the case when only the usual (structure) reflections are taken into consideration. Firstly, simpler mathematical expressions for the description of X-ray scattering by an SL were shown capable of yielding such important parameters as the layer thickness and strain level at the interface. Secondly, the negligible contribution of the layer with a small value of the structural amplitude (GaAs) to the total scattering makes it possible to separate the influence of another SL component. Thirdly, independence of the contribution of the GaAs structural perfection from the general scattering picture makes it possible to determine the structural data of another layer (AlAs) composed of atoms with a larger difference of atomic form factors. In addition, the picture of satellite maxima has richer character as compared with that for the structure reflections, which provides more realistic values of the SL characteristics during the fitting process.

References

- Aleksandrov, P. A., Belova, N. E., Nazarov, S. A., Nefedov, A. A., Fanchenko, S. A., Charlanov, V. A. & Schumilov, D. Yu. (1998). *Surf. Rev. Lett.* **5**, 295–298.
- Afanas'ev, A. M., Chuev, M. A., Imamov, R. M., Lomov, A. A., Mokerov, B. G., Fedorov, Yu. V. & Guck, A. V. (1997). *Krystallografiya*, **42**, 514–521. (In Russian.)
- Asplund, C., Mogg, S., Plaine, G., Salomonsson, F., Chitica, N. & Hammar, M. (2001). *J. Appl. Phys.* **90**, 794–800.
- Bowen, D. K. & Tanner, B. K. (1998). *High-Resolution X-ray Diffractometry and Topography*. London: Taylor and Francis.
- Cockerton, A., Green, G. S. & Tanner, B. K. (1989). *Mater. Res. Soc. Symp. Proc.* **138**, 65–69.
- Datsenko, L. I., Kladko, V. P., Machulin, V. F. & Molodkin, V. B. (2002). *X-ray Dynamic Scattering by Actual Crystals in the Anomalous Dispersion Region*. Kiev: Akadempriodika. (In Russian.)
- Haase, M., Prost, W., Velling, P., Liu, Q. & Tegude, F. J. (1998). *Thin Sol. Films*, **319**, 25–28.
- Holy, V., Kubena, J. & Ploog K. (1990). *Phys. Status Solidi B*, **162**, 347–361.
- Holy, V., Pietch, U. & Baumbach, T. (1998). *High-Resolution X-ray Scattering from Thin Films and Multilayers*. Berlin: Springer.
- Jenichen, B., Hey, R., Wassermeier, M. & Ploog, K. (1997) *Il Nuovo Cimento*, **19**, 454–462.
- Kladko, V. P., Datsenko, L. I., Zytikiewicz, Z., Bak-Misiuk, J. & Maksimenko, Z. V. (2001). *J. Alloys Compd.* **328**, 218–221.
- Kladko, V. P., Datsenko, L. I., Machulin, V. F. & Molodkin, V. B. (2003). *Met. Phys. Adv. Technol.* **25**, 556–564.

- Kladko, V. P., Datsenko, L. I., Kuchuk, A. V., Shalimov, A. V., Domagala, J. & Korchovy, A. A. (2004). *Ukr. J. Phys.* **49**, 75–80.
- Kyutt, R. N., Shubina, T. V., Sorokin, S. V., Solnyshkov, D. D., Ivanov, S. V. & Willander, M. (2003). *J. Phys. D Appl. Phys.* **36**, A166–A171.
- Macranger, A. T., Schwartz, G. P., Gualtieri, G. J. (1988). *J. Appl. Phys.* **64**, 6733–6745.
- Magilyanski, D., Blumin, M., Gartstein, E., Opitz, R. & Kohler, R. (1999). *J. Cryst. Growth*, **198–199**, 1070–1076.
- Punegov, V. I. (1990). *Krystallogr. Rep.* **35**, 576–583.
- Punegov, V. I. (1995). *Physica Solid State*, **37**, 1134–1148. (In Russian.)
- Speriosu, V. S. & Vreelang, T. (1984). *J. Appl. Phys.* **56**, 1591–1600.
- Tapfer, I. & Ploog, K. (1989). *Phys. Rev. B*, **40**, 9802–9810.
- Tran, C. Q., Chantler, C. T., Barnea, Z., Paterson, D. & Cookson, D. J. (2003). *Phys. Rev. A*, **67**, 042716–042722.
- Velling, P., Janßen, G., Agethen, M., Prost, W. & Tegude, F. J. (1998). *J. Cryst. Growth*, **195**, 117–123.